Water Research, Volume 47, Issue 11, 1 July 2013, Pages 3688–3695

Quantifying the loss of methane through secondary gas mass transport (or 'slip') from a micro-porous membrane contactor applied to biogas upgrading

Andrew McLeod, Bruce Jefferson, Ewan J. McAdam*

Cranfield Water Science Institute, Building 39, Cranfield University, Bedfordshire, MK43 0AL, UK
*Corresponding author e-mail: e.mcadam@cranfield.ac.uk

Abstract

Secondary gas transport during the separation of a binary gas with a micro-porous hollow fibre membrane contactor (HMFC) has been studied for biogas upgrading. In this application, the loss or 'slip' of the secondary gas (methane) during separation is a known concern, specifically since methane possesses the intrinsic calorific value. Deionised (DI) water was initially used as the physical solvent. Under these conditions, carbon dioxide (CO_2) and methane (CH_4) absorption were dependent upon liquid velocity (V_L). Whilst the highest CO_2 flux was recorded at high V_L, selectivity toward CO_2 declined due to low residence times and a diminished gas-side partial pressure, and resulted in slip of approximately 5.2 % of the inlet methane. Sodium hydroxide was subsequently used as a comparative chemical absorption solvent. Under these conditions, CO_2 mass transfer increased by increasing gas velocity (V_G) which is attributed to the excess of reactive hydroxide ions present in the solvent, and the fast conversion of dissolved CO_2 to carbonate species reinitiating the concentration gradient at the gas-liquid interface. At high gas velocities, CH_4 slip was reduced to 0.1 % under chemical conditions. Methane slip is therefore dependent upon whether the process is gas phase or liquid phase controlled, since methane mass transport can be adequately described by Henry's law within both physical and chemical solvents. The addition of an electrolyte was found to further retard CH_4 absorption via the salting out effect. However, their applicability to physical solvents is limited since electrolytic concentration similarly impinges upon the solvents capacity for CO_2. This study illustrates the significance of secondary gas mass transport, and furthermore demonstrates that gas-phase controlled systems are recommended where greater selectivity is required.

Keywords: Binary gas; slipping; slippage; fugitive; solvent recirculation; gas/liquid

1. Introduction

Biogas is a renewable source of methane (CH_4) produced on a large scale at wastewater treatment works during anaerobic digestion. Typically the biogas has a CH_4 content of 55-60 % by volume, compared to >90 % CH_4 for natural gas. Carbon dioxide (CO_2) is the key balancing gas contributing 35-50 % of the total gas volume. As an inert gas, CO_2 lowers the calorific value (CV) of the biogas from 36 MJ m^{-3} for natural gas to 21 MJ m^{-3} (Ryckebosch *et al*, 2011). Whilst the lower CV of biogas is appropriate for direct utilisation in combined heat and power (CHP) applications, the CV must be upgraded for use as 'biomethane', or natural gas alternative, principally through the selective separation of the CO_2. As a result of incentivisation schemes, it is increasingly preferable to upgrade biogas for 'gas to grid' instead of electricity generation via CHP because of the disparity in value of the gas for these applications. For example, as a consequence of the 'renewable heat incentive' (RHI) in the UK, a cubic meter of biogas is worth approximately 32 pence (p) if used as a natural gas alternative but only 19 p when applied to CHP (Read *et al*., 2011).

Several technologies exist for selective CO_2 removal, including pressure swing adsorption (PSA), dense membrane separation and absorption columns using either water or a chemical as the absorption solvent. Whilst the specific mechanism for gas separation differs between technologies, these current process options are not able to offer definitive selectivity during separation, thus some loss of the secondary gas can be expected. The term 'slip', corresponds to the loss of this secondary gas, in this case methane, from the product side due to either co-permeation, in the case of dense permeation membranes, or co-dissolution during absorption. The significance of slip to process operation is application specific. For example, in the case of dilute hydrogen sulfide (H_2S) absorption from air for odour treatment (Jefferson *et al.,* 2005; Esquiroz-Molina et al., *In Press*), the co-solubilisation of the ternary gases nitrogen and oxygen (and low concentration CO_2) are not quantified, or considered. However, for biogas upgrading the significance of methane 'slip' is considerable since methane possesses the intrinsic value as the product gas. Few published studies have sought to quantify slip. Early studies of full-scale dense gas membranes for CH_4 recovery from

landfill gas reported up to 18 % methane slip (Ho and Sirkar, 1992) though this has since been reduced using multiple membrane arrays to enable subsequent treatment of the retentate gas stream which comprises low concentration methane. By comparison, 8 % and 13.1 % CH_4 slip have been reported for PSA and absorption respectively, the latter using water as the solvent and a pressurised gas phase of between 20-25 bar (Baldwin, 2011; Läntelä *et al*., 2011).

For biogas upgrading at sewage works, packed tower absorption is the predominant technology employed with water used as the absorption solvent, for process simplicity, and due to the wide availability of treated final effluent onsite. Water demonstrates a reasonable selectivity for CO_2 since methane is only a partially soluble gas. Consequently, analysis of methane transport during process evaluation is often neglected. However, high liquid flow rates are demanded in absorption technologies that result in high methane slip over long operational periods. Several authors have considered the application of hollow fibre membrane contactors (HFMCs) as an alternative absorption technology to conventional packed towers for biogas upgrading (Atchariyawut et al., 2007; Simons et al., 2009). The hydrophobic membrane enables separation of the gas and liquid phases, with gaseous diffusion facilitated through the micro-porous membrane which enhances mass transfer and increases specific surface area availability compared to conventional absorbers. Consequently, Nii and Takeuchi (1992) noted an order of magnitude reduction in liquid flow rate when comparing a polydimethylsiloxane HFMC with a conventional packed absorption column to achieve comparable removal of CO_2 from flue gas. Whilst enhanced mass transfer has been ascertained, the fate of the secondary gas, or the slip, during absorption has not been examined and is central to understanding process efficacy. This study therefore seeks to quantify: (i) the mass transfer of the two principal biogas components methane and carbon dioxide to determine the significance of methane slip from HFMC applied to upgrading; (ii) the capacity to mitigate methane slip through manipulating solvent chemistry; and (iii) evaluating the impact of multiple solvent cycles on methane slip compared to single pass operation.

2. Materials and methods

2.1 Equipment setup and operation

Methane (99.995 %) and carbon dioxide (99.7 %) (BOC gases, Ipswich, UK) gases were controlled using mass flow controllers (0.01-1.0 L min^{-1}, Roxspur Measurement and Control Ltd., Sheffield, UK) and were mixed in-line to provide an initial 60/40 CH_4/CO_2 gas composition to the shell-side of the HFMC (Liqui-Cel® 1.7x5.5 MiniModule®, Membrana GmbH, Wuppertal, Germany)(Figure 1). The outlet gas flow rate was measured using a bubble flow meter (50 mL, Restek, Bellefonte, USA). Absorbent was stored in a 50 L PVC tank and maintained at 24-26 °C by a thermostat circulator (GD120, Grant Instruments Cambridge Ltd., Shepreth, UK) sited in the water bath. The absorbent was passed through the fibre lumen in counter-current mode using a centrifugal pump (max. 6 L min^{-1}, 50010 series, Jabsco GmbH, Norderstedt, Germany). The HFMC comprised 7400 polypropylene (PP) fibres, with a nominal outer diameter (OD) and length of 300 µm and 0.113 m respectively, yielding a surface area of 0.58 m^2 (based on inner fibre diameter, ID of 220 µm). The fibres were characterised with a nominal pore size of 0.03 µm and porosity of 40 %. The fibres were potted in polyurethane fixed in a polycarbonate shell with an ID of 0.0425 m resulting in a packing density of 0.369.

Solvent recirculation was investigated to compare multiple passes (or cycles) of solvent use to single pass solvent use. For these experiments, a 10 L absorbent reservoir was incorporated into the liquid side of the experimental design to minimise the impact of sampling from the liquid phase on the resultant mass transfer data. The vessel was magnetically stirred to ensure complete mixing of the bulk solvent. During multiple-pass (MP) experiments, a smaller HFMC was employed to ensure that the MP tests could be conducted with a reasonably short timeframe. This smaller module (Liqui-Cel® 1x5.5 MiniModule®, Membrana GmbH, Wuppertal, Germany) comprised of 2300 identical hollow fibres (OD 300 µm/ ID of 220 µm/pore size 0.03 µm) but 0.10 m in length, yielding a surface area of 0.18 m^2.

109 *2.2 Preparation and sampling*

110 All absorbents were based on de-ionised (DI) water with a resistivity of 18.2 MΩ-cm. For
111 experiments using chemically based solvents, either sodium chloride (NaCl) or sodium hydroxide
112 (NaOH) was used (NaCl 99% and NaOH 98% pellets, Fisher Chemicals, Loughborough, UK). Chemical
113 solutions were initially prepared as concentrates by adding 1755 g NaCl and/or 1320 g NaOH to 10 L
114 of DI water with thorough mixing to ensure complete dissolution. Concentrates were then diluted in
115 the absorbent tank to provide 1.0 M solutions. To determine liquid phase concentrations, the
116 method adapted from Alberto *et al.*, (2000) was used in which evacuated vials were employed to
117 ensure no exposure of aqueous solvent samples to the environment. Prior to use, the 22.7 mL GC-
118 MS glass vials were capped and sealed with gas-tight PTFE/aluminium crimp caps (Fisherbrand,
119 Fisher Scientific, Loughborough, UK). Vials were then evacuated for 20 s using a vacuum pump
120 (CAPEX L2C, Charles Austen Pumps, Byfleet, Surrey, UK) at fixed pressure to ensure consistent
121 vacuum pressures in each vial (0.3 atm). Aqueous solvent samples were collected from a luer lock
122 needle fitted on the liquid outlet. The reduced vial pressure imposed a vacuum on the liquid side
123 enabling collection of a liquid sample, which when complete, had equilibrated to atmospheric
124 pressure. Liquid samples were agitated for 7 minutes (maximum speed, Multi Reax, Heidolph,
125 Schwabach, Germany), and were subsequently left to equilibrate overnight. The resultant dissolved
126 phase concentrations were calculated based on a mass balance (Alberto et al., 2000). Methane flux
127 was calculated using:

128 $$J_{CH4} = \frac{\left(Q_{l,i} \times c_f\right) - \left(Q_{l,0} \times c_r\right)}{M_{r,CH4} \times A_m} \quad \text{(equation 1)}$$

129 Where J_{CH4} is methane flux (mol m^{-2} s^{-1}), $Q_{l,i}$ and $Q_{l,0}$ are the inlet and outlet liquid flow rates
130 respectively (m^3 s^{-1}), c_f and c_r are CH_4 concentrations in the liquid feed and retentate respectively (g
131 m^{-3}), $M_{r,CH4}$ is the relative molecular mass of methane and A_m is the active surface area of the HFMC.
132 Gas samples were taken from GC septa fitted on the gas-side upstream and downstream of the

contactor and injected onto a gas chromatograph. The CO_2 flux was calculated according to Atchariyawut *et al.* (2007):

$$J_{CO2} = \frac{\left[\left(Q_{gi} \times c_f\right) - \left(Q_{go} \times c_r\right) \times 273.15 \times 1000\right]}{22.4 \times T_g \times A_m} \quad \text{(equation 2)}$$

Where J_{CO2} is the CO_2 flux (mol m^{-2} s^{-1}), Q_{gi} and Q_{go} are the inlet and outlet gas flow rates respectively (m^3 s^{-1}), c_f and c_r are the CO_2 mole fraction in the gas feed and gas retentate respectively, T_g is the gas temperature (K) and A_m is the active surface area (m^2). Selectivity was calculated using (Rongwong *et al.*, 2011; Lu *et al*., 2006):

$$Selectivity = \frac{R_{CO2} / R_{CH4}}{F_{CO2} / F_{CH4}} \quad \text{(equation 3)}$$

Where R_{CO2} and R_{CH4} are the CO_2 and CH_4 concentrations in the retentate liquid (g L^{-1}), and F_{CO2} and F_{CH4} are the CO_2 and CH_4 concentrations in the gas feed (g L^{-1}). All samples were analysed in triplicate.

2.3 Analysis

A gas chromatograph (GC) fitted with a thermal conductivity detector (TCD) was used to analyse the gas and liquid samples (200 Series GC-TCD Cambridge Scientific Instruments Ltd., Witchford, UK). Gas solutes were separated on an Alltech® CTR I concentric packed column which has a concentric column with a 1/4“ outer column surrounding an 1/8“ inner column (Alltech Associates Inc., Deerfield, Illinois, USA). Samples were introduced onto the column in a 1mL volume and eluted using Helium as the carrier gas at an entry pressure of 4.2 bar(g). The isothermal method used an injector temperature of 150 °C, an oven temperature of 30 °C and a detector temperature of 180 °C. The instrument was calibrated using certificated CO_2 and CH_4 gas standards (Scientific Technical Gases Ltd., Staffordshire, UK) prior to each analysis. A sharp methane peak eluted from the inner column containing mixed porous polymer packing at a retention time of 30 s followed by the CO_2 peak at 90 s. Concentration of chemically absorbed CO_2 in NaOH containing solutions, existing as carbonate,

was ascertained by titration of retentate absorbent with 1.0 M HCl using $BaCl_2$ to neutralise the carbonate ions (Benedetti-Pichler Cefola, 1939).

3. Results

3.1 Impact of solvent chemistry on biogas component flux

A CO_2 flux of $7.6x10^{-5}$ mol m^{-2} s^{-1} was recorded when using DI water as the absorption solvent, at a fixed V_G of 0.0047 m s^{-1} and V_L of 0.0054 m s^{-1}, which corresponded to an L/G of 1.15, with a Reynolds number (*Re*) of 1.32 (Figure 2a). The L/G was progressively increased by increasing V_L to a maximum of 0.024 m s^{-1} (*Re* = 5.90), upon which a CO_2 flux of $1.7x10^{-4}$ mol m^{-2} s^{-1} was recorded, representing an increase in CO_2 flux of approximately 200%. Analogous behaviour was observed for CO_2 flux when NaCl was added as a simple electrolyte, where V_L ranged from 0.0074 m s^{-1} (*Re* = 1.71) to 0.022 m s^{-1} (*Re* = 5.12). *Re* values for the gas on the shell side ranged between an initial *Re* = 10.5 (accounting for viscosity of initial gas mixture and V_G of 0.0047 m s^{-1}; Jackson, 1956) to a minimum *Re* = 4.2 (accounting for change in gas mixture composition and V_G) at the HFMC outlet for DI solvent. Substitution of the DI and NaCl 'physical' solvents for a 1 M NaOH 'chemical' absorbent resulted in a CO_2 flux of $2.98x10^{-4}$ and > 99 % CH_4 concentration in the outgas, which remained unchanged when V_L was varied from 0.0122 m s^{-1} (*Re* = 2.47) to 0.0242 m s^{-1} (*Re* = 4.90). This corresponded to a plateau in CO_2 flux with increasing V_L, indicating that the process was gas phase controlled (Li and Chen, 2005; Esquiroz-Molina, In Press). Gas velocity (V_G) was subsequently increased from 0.0047 m s^{-1} to a maximum of 0.031 m s^{-1} at a fixed V_L of 0.0089 m s^{-1} to reduce the L/G ratio and identify the impact upon CO_2 flux (Figure 2b). CO_2 flux was found to be dependent upon V_G, with the highest CO_2 flux of $1.74x10^{-3}$ mol m^{-2} s^{-1} recorded at a V_G of 0.031 m s^{-1}. Similarly to DI water, no quantifiable difference in CO_2 flux could be noted following the inclusion of NaCl to NaOH. Since both physical and chemical systems were ostensibly controlled by differing phases, direct comparison is difficult to ascertain. However, both V_L (0.009 m s^{-1}) and V_G (0.0047 m s^{-1}) were identical for DI and NaOH at an L/G of 1.92 which corresponded to the minimum CO_2 flux of $2.98x10^{-}$

^{4} mol m^{-2} s^{-1} recorded for the chemical solvent. The flow regime for gas in the shell side during variable V_G experiments using NaOH absorbents was relatively consistent with that observed for DI experiments where V_G was fixed. *Re* = 70 represents the greatest possible value, for an initial gas mixture and maximum V_G of 0.031 m s^{-1}, although this declines with loss of V_G and change in composition via rapid CO_2 absorption by NaOH.

The highest CH_4 flux was recorded using DI water. At an L/G of 1.15, CH_4 flux was $2.03x10^{-6}$ mol m^{-2} s^{-1} which increased to a maximum flux of $1.15x10^{-5}$ mol m^{-2} s^{-1} at an L/G of 5.2 (Figure 3). Methane flux diminished markedly with the inclusion of NaCl to DI water. To illustrate, a CH_4 flux of $6.2x10^{-6}$ mol m^{-2} s^{-1} was recorded at L/G 4.7 compared to $8.6x10^{-6}$ mol m^{-2} s^{-1} for DI water at the lower L/G of 4.2. For the NaOH solvent, CH_4 fluxes were comparable to those of NaCl below L/G 2.6. However, at L/G greater than 2.6, CH_4 flux recorded for the NaOH solvent apparently increased as an exponent of L/G, subsequently recording a CH_4 flux of $9.7x10^{-6}$ mol m^{-2} s^{-1} at L/G 5.2, only 15 % below that observed for DI water. Addition of NaCl to NaOH introduced the greatest limitation to CH_4 flux, recording between $8.9x10^{-7}$ and $4.6x10^{-6}$ mol m^{-2} s^{-1} for L/G ranging 1.4 to 5.

Following process optimisation using the rate limiting phase (V_G in the case of chemical based solvents NaOH and NaOH/NaCl; and V_L for the physical solvents DI water and aqueous NaCl), selectivity toward CO_2 was estimated for each solvent (Figure 4). For physical solvents, selectivity was greater when using NaCl. However, a linear decrease toward CO_2 selectivity was noted for both solvents when V_L was increased. For example, for DI water, selectivity decreased from 166 at L/G 2.4 to 106 at L/G 5.2. The NaCl/NaOH solvent increased selectivity for CO_2 at L/G 0.29 from 1030 for NaOH to 2250. At higher L/G, selectivity diminished to that observed for physical solvents.

Data was selected from the reported datasets to enable an approximate comparison of slip, from the solvents evaluated. To normalise the datasets, an outlet gas composition of 85 % methane, equivalent to North Sea natural gas (Persson et al., 2006), was selected (Table 1). The highest slip was observed when using DI water at 5.2 %. In comparison, the chemical solvent reduced methane

slip to 0.1 %. Adding the NaCl electrolyte reduced methane slip in both physical and chemical solvents to 4.0 % and 0.03 % respectively.

3.2 Application of solvent recirculation to minimise slip

Single pass solvent use was compared to recirculating the solvent in multi-pass (MP) to enable greater utilisation of the available solvent (Figure 5). Cumulative losses were compared following subsequent solvent uses (without regeneration) based upon a parameter normalised to CO_2 removal (CH_4 lost per gram CO_2 absorbed, g g^{-1}). For both solvents, a pseudo-plateau was evidenced following one recirculation which can be explained by the saturation of the solvent with CH_4 after one circulation. This is supported by the measured dissolved phase methane concentration which stabilised following approximately one recirculation. However, methane losses were lower using the NaOH solvent. For example, following two solvent recirculations, losses were 0.086 g g^{-1} and 0.709 g g^{-1} for the NaOH and DI solvents respectively. Over five solvent recirculations, the chemical solvent supported an outlet gas phase concentration of >99% CH_4 (Figure 6). In contrast, outlet gas quality rapidly diminished for the DI solvent following less than one use.

4. Discussion

A significant finding in this study was that methane slip was dependent upon whether the process was gas phase or liquid phase controlled. For physical solvents such as DI water, the liquid phase presented the rate limiting condition to CO_2 mass transfer. This manifested as an increase in CO_2 flux, and therefore an enhancement in gas-side methane purity, when V_L was increased. The DI solvent approached saturation for CH_4 at low V_L. This can be explained by the partial solubility of methane in water, yielding a predicted saturation concentration of 13.5 mg L^{-1} at a partial pressure of 60 % (Willhelm et al., 1977). A proportionate increase in methane flux was subsequently observed with an increase in V_L and can be explained by the continual saturation of newly introduced solvent at the solvent-membrane boundary. In contrast, dissolved CO_2 concentration diminished at high V_L

from a maximum of 500 mgCO_2 L^{-1} at V_L 0.011 m s^{-1}, to 387 mgCO_2 L^{-1} at V_L 0.024 m s^{-1}. This can be explained by a combination of the lower residence time available for absorption which limited radial gas transport from the solvent-membrane boundary due to under-developed laminar flow conditions (*Re* << 2100) observed throughout for DI water (Re_{max} = 5.90) (Dindore *et al.*, 2005), and a reduction in gas-side CO_2 partial pressure at higher V_L. This reduction in CO_2 solvent concentration subsequently reduced selectivity toward CO_2 with an increase in V_L (Figure 4). The hydrodynamic conditions were comparable for all solvents across the V_L ranges examined, with insufficient difference in viscosity and density of electrolytic solutions for any significant change in flow regime (Zhang *et al.,* 1996; Sipos *et al*., 2000; Laliberte, 2007).

For the chemically reactive NaOH solvent, the process was gas phase controlled, which is illustrated by the negligible gradient recorded for CO_2 flux following an increase in V_L (Figure 2a). This chemical reaction is described as 'fast' (11,000 m^3 $kmol^{-1}$ s^{-1}), such that dissolution can no longer be predicted by Henry's Law, as upon penetration the CO_2 reacts to form bicarbonate (HCO_3^-) (Kucka *et al*., 2002; Pohoricki and Moniuk, 1988). Consequently, whilst operated within the low *Gz* number range applied to physical solvents, this conversion to carbonate species, in the presence of a high reactant concentration, was sufficient to re-establish the concentration gradient at the membrane-solvent boundary. The excess of reactive [OH^-] within the reaction zone further enabled a reduction in the operational L/G ratio. This limited CH_4 flux, as the physical dissolution of CH_4 in NaOH can be similarly described by Henry's law and is thus attributable to solvent flow rate. To illustrate, to achieve an equivalent outlet CH_4 purity of 85 %, the L/G required for DI and NaOH solvents were 5.2 and 0.33 yielding 'slip' of 5.2 % and 0.1 % respectively. Interestingly, when using the chemical solvent at L/G >1, the gas-side CO_2 concentration was reduced to below the limit of detection and was coincident with a non-linear increase in methane flux (Figure 3). It is posited that this CH_4 flux enhancement arises from the increase in gas-side CH_4 partial pressure suggesting that an optimum L/G should be identified to limit 'slip' in addition to gas-side CO_2.

Selectivity was enhanced in both chemical and physical absorption systems by the inclusion of NaCl (Figure 4). The NaCl behaved as an electrolyte, which induced 'salting out' of the physically absorbed gas species resulting in a reduction in the attainable saturation constant. Setschenow (1889) supposed that 'salting out' was induced by a preference of water molecules to hydrate and dissolve ionic species rather than the uncharged gas candidates. Latterly Masterton and Lee (1970) used 'scaled particle theory' (SPT) to suggest that salting out increased the work required to form a cavity (within the condensed liquid phase) of sufficient size to accommodate a gas solute. Consequently, electrolyte addition to the physical solvent (DI) reduced methane slip to 4 % compared to 5.2 % for DI water. The use of NaCl to improve outlet gas quality was also assessed by Atchariyawut *et al*. (2007). The authors based the improvement in outlet gas quality on the electrolytes capacity to reduce water vapour content. Whilst the author's hypothesis of reduced water activity is valid, clearly the contribution of reduced methane 'slip' must also be considered.

Due to the inclusion of NaCl, the CO_2 saturation constant was reduced by 22 %. However, the measured dissolved CO_2 concentration was below this saturation concentration and hence the impact on CO_2 flux was seemingly negligible (Figure 2a). It is posited that further lowering of the solubility constant will impede absorption performance. Interestingly, whilst the chemical solvent reduced slip through enabling lower L/G operation, NaOH similarly dissociates into ionic form, presenting a synergistic effect since slip is therefore also retarded through salting out of the [Na^+] and [OH^-] ions (Weisenberger and Schumpe, 1996), and is supported by the diminished CH_4 flux recorded for NaOH when compared to DI (Figure 3). Consequently, the addition of NaCl to NaOH absorbent effectively doubled the electrolytic solvent concentration, further inhibiting CH_4 flux and subsequently enhanced selectivity for CO_2 by approximately 200 %. Since the chemical solvent's reactivity offsets the lower physical absorption constant for CO_2, it is suggested that higher electrolytic concentrations can be implemented and methane 'slip' further decreased.

Using multi-pass absorption enables further cessation of 'slip' since both physical and chemical solvents are essentially saturated with CH_4 in a single pass, thus subsequent solvent

285 recirculation should retard further CH_4 flux, tending measured CH_4 flux to zero. However, the
286 capacity to utilise physical solvents in multi-pass absorption is limited as approximately 50 % of the
287 maximum CO_2 load is also reached in single-pass. In comparison, the CO_2 flux and outlet gas quality
288 recorded for the chemical solvent following five recirculations was analogous to single pass,
289 demonstrating a sustained excess of highly reactive hydroxide [OH^-] ions. Based on an idealised
290 stoichiometric conversion of 2:1, [OH^-]: CO_2 (Vas Bhat *et al*., 2000) and an L/G of 5.2, approximately
291 37 chemical solvent recirculations are possible before reaching a [OH^-] concentration of 0.1 M.
292 Interestingly, whilst an order of magnitude lower in chemical concentration, 0.1 M NaOH has been
293 shown sufficient to maintain a >99 % CH_4 outlet gas concentration under analogous hydrodynamic
294 conditions (Galan-Sanchez, 2011).
295 Physical absorption in HFMC demonstrated methane slip of 5.2 %. Although direct comparison to
296 conventional water scrubbers cannot be made due to differences in gas-side preconditioning and
297 scale, this is markedly lower than the 13.1% slip recorded for a pilot scale unit applied to landfill gas
298 (Läntelä *et al*., 2011) and is ostensibly a function of lower solvent consumption; an observation
299 which is supported by previous authors (Nii and Takeuchi, 1992; Herzog and Pederson, 2000). Lower
300 'slip' values of 4 % to 5 % have been recorded for full-scale water scrubbers, though it is unclear
301 whether the balance includes the use of abatement technologies such as thermal oxidisers which
302 oxidise the slipped methane to CO_2 (Patterson *et al.*, 2011; Wolf and Nettelnbreker, 2011). In
303 addition, to the financial significance of enhancing the recovery of biomethane through minimising
304 slip, financial incentivisation now also rewards installations which operate at 'slip' below 0.5 % (Wolf
305 and Nettelnbreker, 2011). Based on this study, to reach this target without the use of abatement
306 technologies, chemical solvents are required as this enables the shift to gas-phase control which
307 minimises 'slip' through minimum solvent consumption; though the energy penalty associated with
308 solvent regeneration must also be considered. The characteristically low absorbent demand of
309 HFMCs could conceivably limit the energy necessary for chemical regeneration through a reduction
310 in liquid volume, which is also coupled to a significantly reduced pumping requirement. This is in

addition to the revenue from the methane that would otherwise have been lost at higher slip. For example, assuming biogas production of 1000 m^3 $hour^{-1}$ (a moderate full-scale flow rate) with 60 % initial CH_4 content, an upgrading plant operating at 5.2 % slip would lose approximately £87,500 $year^{-1}$ at 32 p m^{-3}. In contrast, a NaOH solvent with 0.1 % slip would only lose £1,700 $year^{-1}$. Only £500 $year^{-1}$ would be lost at 0.03 % slip in a NaOH + NaCl absorbent.

In practice, there is a trade-off between CAPEX and OPEX, such that the application of highly reactive chemical solvents will be used to reduce asset scale by increasing throughput, consequently, the number of achievable solvent recirculations could be lower than presented in this study. However, both energy and carbon returns demonstrate that operation greater than one recirculation is sufficient to derive a net energy benefit through minimising methane slip (Figure 7). A criticality in L/G was also demonstrated where unnecessary operation at L/G >1 could impinge upon methane losses. This underpins a tacit advantage of HFMCs versus conventional packed columns in that the latter are operationally limited to turnup/turndown during process perturbation such as inlet gas composition or flow variation. By comparison HFMCs can achieve more rapid transitions in V_L due to phase separation which enables HFMCs to operate at minimum V_L and thus limit further 'slip'.

5. Conclusion

The significance of methane slip during biogas upgrading was dependent upon whether the process was gas phase or liquid phase controlled since methane transport was governed by Henry's law and hence independent of chemical reactivity.

- For physical solvents, absorption was dependent upon V_L. However, at high VL, selectivity toward CO2 declined due to low residence times and an underdeveloped regime;
- For chemical solvents, CO_2 mass transfer was dependent upon V_G which was driven by an excess of [OH^-] ions available in the solvent for chemical reaction;

- Electrolytes can retard CH_4 absorption via the salting out effect. In physical solvents, electrolytic concentration is limited by the effect upon CO_2 solubility. However, in chemical solvents, CO2 absorption is decoupled from physical constants, thus an excess of electrolyte can enhance selectivity further; and
- Multi-pass chemical solvent recirculation enables further methane slip prevention. Initial saturation of the solvent for CH_4, ensures that CH_4 flux tends toward zero following subsequent uses for CO_2.

Acknowledgments

The authors would like to thank the Engineering and Physical Sciences Research Council (EPSRC, V/N: 08001923), Anglian Water, Northumbrian Water, Severn Trent Water and Yorkshire Water for their financial support.

References

Alberto, M.C.R., Arah, J.R.M., Neue, H.U., Wassmann, R., Lantin, R.S., Aduna, J.B., Bronson, K.F., 2000. A sampling technique for the determination of dissolved methane in soil solution. Chemosphere 2 (1), 57-63.

Atchariyawut, S., Jiraratananon, R., Wang, R., 2007. Separation of CO_2 from CH_4 by using gas-liquid membrane contacting process. Journal of Membrane Science 304 (1-2), 163-172

Baldwin, J., 2011. Biomethane market opportunities. Rushlight Events: Commercial issues and technology developments in organic waste investments. 22nd February, London, UK

Benedetti-Pichler, A.A., Cefola, M., 1939. Warder's method for the titration of carbonates. Industrial & Engineering Chemistry Analytical Edition 11 (6), 327-332.

Dindore, V.Y., Brilman, D.W.F., Versteeg, G.F., 2005. Hollow fiber membrane contactor as a gas-liquid model contactor. Chemical Engineering Science 60 (2), 467-479.

361 Esquiroz-Molina, A., Georgaki, S., Stuetz, R., Jefferson, B., McAdam, E.J. (Accepted), Influence of pH
362 on gas-phase controlled mass transfer in a membrane contactor for hydrogen sulphide
363 absorption, Journal of Membrane Science (10.1016/j.memsci.2012.10.005).
364 Falk-Pedersen, O., Dannström, H., 1997. Separation of carbon dioxide from offshore gas turbine
365 exhaust. Energy Conversion and Management 38 (1), S81-S86.
366 Galan-Sanchez, I., 2011. Enhancing Energy Production from Gas Engines used for Landfill
367 Applications. MSc Thesis, Cranfield Water Science Institute, Cranfield University.
368 Ho, W.S., Sirkar, K.K., 1992. Membrane Handbook, *Kluwer Academic Publishers*, 91-92.
369 Jefferson, B., Nazareno, C., Georgaki, S., Gostelow, P., Stuetz, R. M., Longhurst, P., Robinson, T.,
370 2005. Membrane gas absorbers for H2S removal - Design, operation and technology
371 integration into existing odour treatment strategies. Environmental technology 26 (7), 793-
372 804.
373 Kreulen, H., Smolders, C.A., Versteeg, G.F., Van Swaaij, W.P.M., 1993. Microporous hollow fibre
374 membrane modules as gas-liquid contractors. Part 1. Physical mass transfer processes. A
375 specific application: Mass transfer in highly viscous liquids. Journal of Membrane Science 78
376 (3), 197-216.
377 Kucka, L., Kenig, E.Y., Górak, A., 2002. Kinetics of the gas-liquid reaction between carbon dioxide and
378 hydroxide ions, Industrial and Engineering Chemistry Research 41 (24), 5952-5957.
379 Kumar, P.S., Hogendoorn, J.A., Feron, P.H.M., Versteeg, G. F., 2002. New absorption liquids for the
380 removal of CO_2 from dilute gas streams using membrane contactors. Chemical Engineering
381 Science 57 (9), 1639-1651.
382 Kumar, P.S., Hogendoorn, J.A., Feron, P.H.M., Versteeg, G.F., 2003. Approximate solution to predict
383 the enhancement factor for the reactive absorption of a gas in a liquid flowing through a
384 microporous membrane hollow fiber. Journal of Membrane Science 213 (1-2), 231-245.

385 Läntelä, J., Rasi, S., Lehtinen, J., Rintala, J., 2011. Landfill gas upgrading with pilot-scale water
386 scrubber: Performance assessment with absorption water recycling. Applied Energy 92 (1),
387 307-314.
388 Li, J.-L., Chen, B.-H., 2005. Review of CO_2 absorption using chemical solvents in hollow fiber
389 membrane contactors. Separation and Purification Technology 41 (2), 109-122.
390 Lu, J., Zheng, Y., He, D., 2006. Selective absorption of H_2S from gas mixtures into aqueous solutions
391 of blended amines of methyldiethanolamine and 2-tertiarybutylamino-2-ethoxyethanol in a
392 packed column. Separation and Purification Technology 52 (2), 209-217.
393 Masterton, W.L., Lee, T.P., 1970. Salting coefficients from scaled particle theory. Journal of Physical
394 Chemistry 74 (8), 1776-1782.
395 Nii, S., Takeuchi, H., 1992. Removal of CO_2 by gas absorption across a polymeric membrane. Journal
396 of Chemical Engineering of Japan 25 (1), 67-72.
397 Nijsing, R.A.T.O., Hendriksz, R.H., Kramers, H., 1959. Absorption of CO_2 in jets and falling films of
398 electrolyte solutions, with and without chemical reaction. Chemical Engineering Science 10
399 (1-2), 88-104.
400 Patterson, T., Esteves, S., Dinsdale, R., Guwy, A., 2011. An evaluation of the policy and techno-
401 economic factors affecting the potential for biogas upgrading for transport fuel use in the
402 UK. Energy Policy 39 (3), 1806-1816.
403 Persson M., Jonsson, O., Wellinger, A., 2007. Task 37 – Biogas upgrading to vehicle fuel standards
404 and grid injection. IEA Bioenergy, 20-21.
405 Pohorecki, R., Moniuk, W., 1988. Kinetics of reaction between carbon dioxide and hydroxyl ions in
406 aqueous electrolyte solutions. Chemical Engineering Science 43 (7), 1677-1684.
407 Qi, Z., Cussler, E.L., 1985. Microporous hollow fibers for gas absorption. II. Mass transfer across the
408 membrane. Journal of Membrane Science 23 (3), 333-345.

409 Rongwong, W., Boributh, S., Assabumrungrat, S., Laosiripojana, N., Jiraratananon, R., 2012.
410 Simultaneous absorption of CO_2 and H_2S from biogas by capillary membrane contactor.
411 Journal of Membrane Science 392–393, 38-47.
412 Ryckebosch, E., Drouillon, M., Vervaeren, H., 2011. Techniques for transformation of biogas to
413 biomethane. Biomass and Bioenergy 35 (5), 1633-1645.
414 Setschenow, J. Z., 1889. Uber Die Konstitution Der Salzlosungenauf Grund Ihres Verhaltens Zu
415 Kohlensaure. Zeitschrift für Physikalische Chemie 4, 117–125.
416 Simons, K., Nijmeijer, K., Wessling, M., 2009. Gas–liquid membrane contactors for CO_2 removal.
417 Journal of Membrane Science 340, 214-220.
418 Stern, S.A., Krishnakumar, B., Charati, S.G., Amato, W.S., Friedman, A.A., Fuess, D.J., 1998.
419 Performance of a bench-scale membrane pilot plant for the upgrading of biogas in a
420 wastewater treatment plant. Journal of Membrane Science, 151 (1), 63-74.
421 Vas Bhat, R.D., Kuipers, J.A.M., Versteeg, G.F., 2000. Mass transfer with complex chemical reactions
422 in gas-liquid systems: Two-step reversible reactions with unit stoichiometric and kinetic
423 orders. Chemical Engineering Journal 76 (2), 127-152.
424 Wang, R., Zhang, H.Y., Feron, P.H.M., Liang, D.T., 2005. Influence of membrane wetting on CO_2
425 capture in microporous hollow fiber membrane contactors. Separation and Purification
426 Technology 46 (1-2), 33-40
427 Weisenberger, S., Schumpe, A., 1996. Estimation of Gas Solubilities in Salt Solutions at Temperatures
428 from 273 K to 363 K. AIChE Journal 42 (1), 298-300.
429 Wilhelm, E., Battino, R., Wilcock, R.J., 1977. Low-pressure solubility of gases in liquid water. Chemical
430 reviews 77 (2), 219-262.
431 Wolf M., Nettelnbreker U., 2011. Method for Biogas Treatment and Biogas Installation. United States
432 patent Application publication, US20110245572.

433 Zhang, H.-Y., Wang, R., Liang, D.T., Tay, J.H., 2006. Modeling and experimental study of CO_2
434 absorption in a hollow fiber membrane contactor. Journal of Membrane Science 279 (1-2),
435 301-310.

436

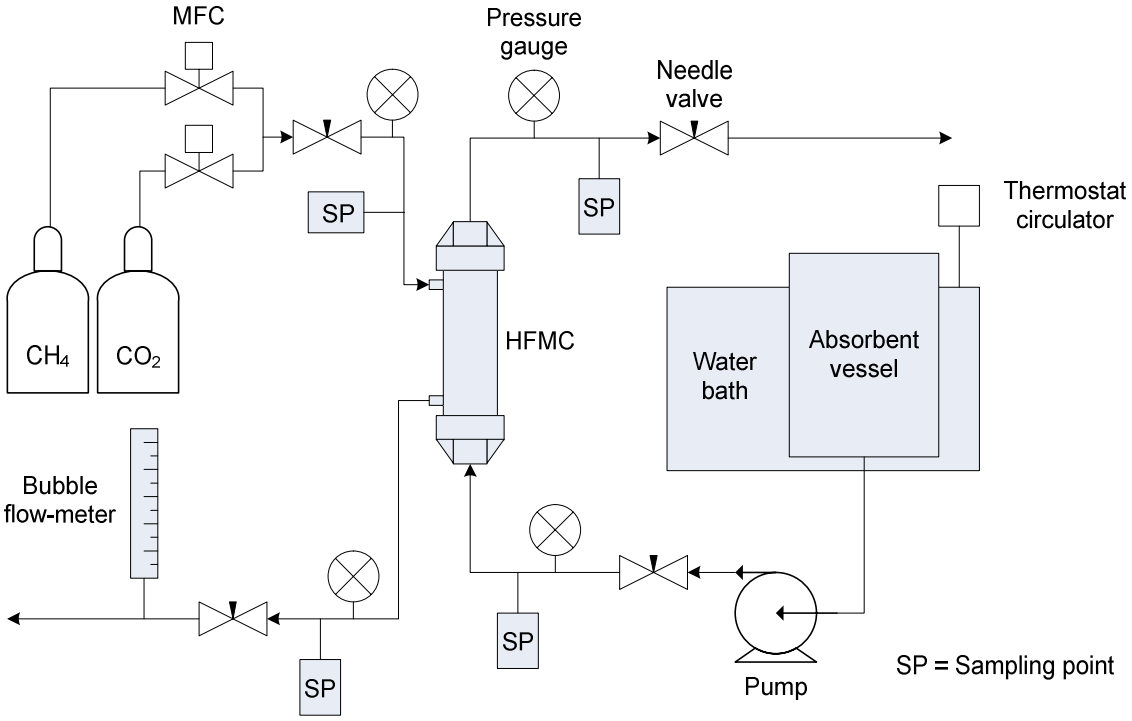

Figure 1. Schematic of the experimental set-up used for determining 'slip' from a polypropylene microporous hollow fibre membrane contactor (HFMC, 0.03 µm pore size).

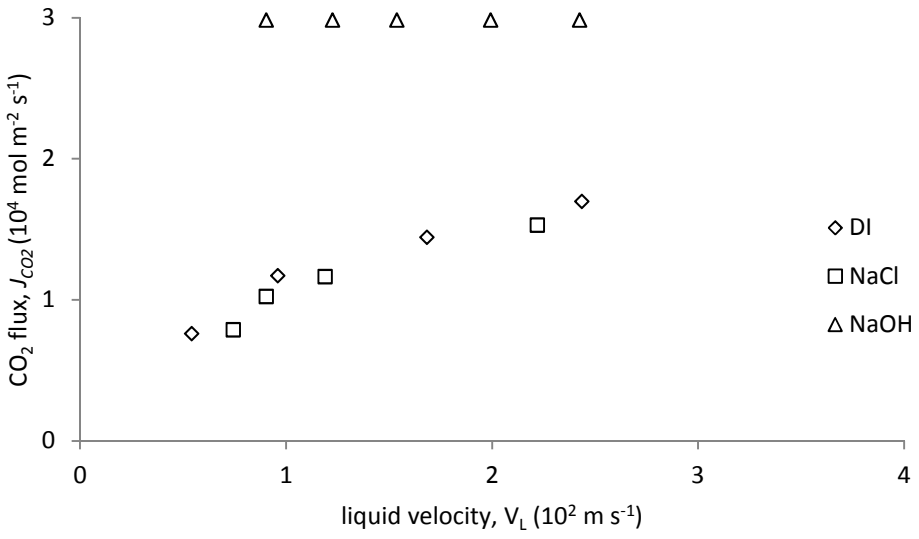

(a)

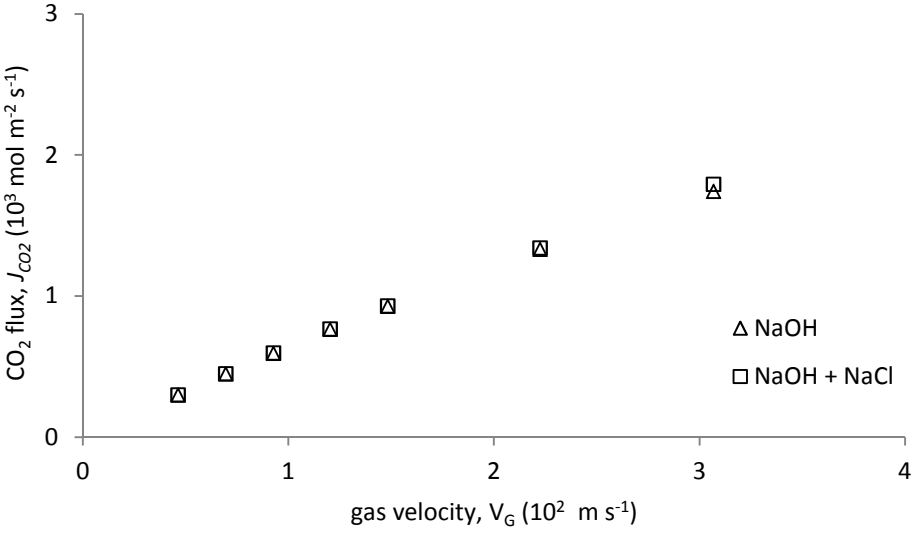

(b)

Figure 2. (a) Impact of liquid velocity (V_L 0.0054 m s^{-1} to 0.024 m s^{-1}) with fixed initial gas velocity (V_G 0.0047 m s^{-1}) on CO_2 flux in DI, NaCl, and NaOH absorbents fixed at 24-26 ˚C (b) Impact of gas velocity (V_G 0.0017 m s^{-1} to 0.031 m s^{-1}) with fixed liquid velocity (V_L 0.0089 m s^{-1}) on CO_2 flux in NaOH and NaOH + NaCl absorbents fixed at 24-26 ˚C

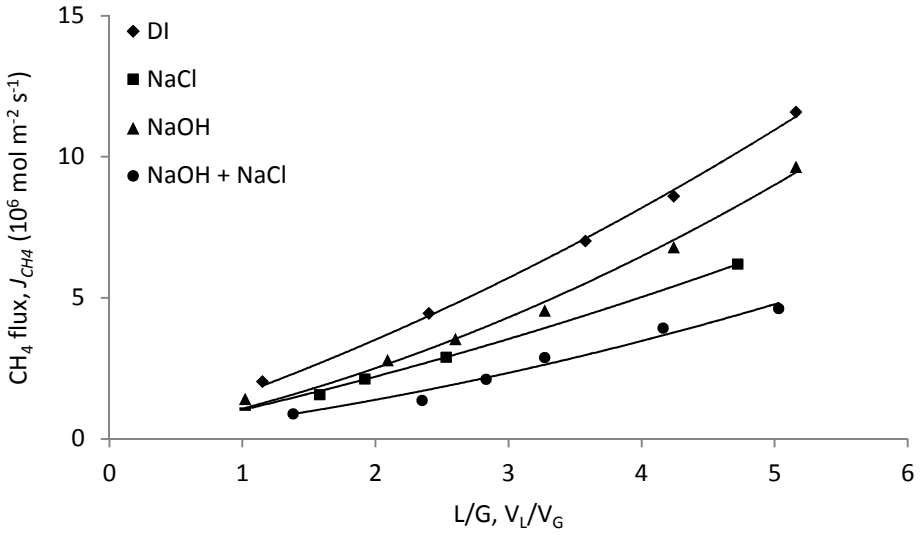

Figure 3. The impact of liquid velocity (V_L 0.0046 m s^{-1} to 0.024 m s^{-1}) on CH_4 flux in four solvents DI, NaCl, NaOH, and NaOH/NaCl. Absorbent solvent temperature fixed at 24-26 ˚C.

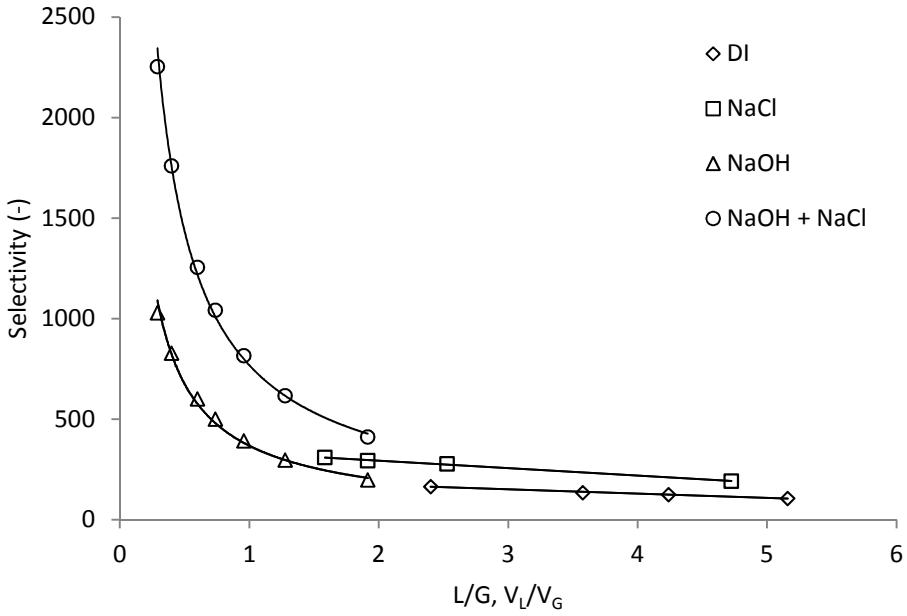

Figure 4. Influence of hydrodynamic conditions on CO_2 selectivity. Liquid velocity (V_L) varied from 0.0074 m s^{-1} to 0.024 m s^{-1} for DI and NaCl solvents and gas velocity (V_G) fixed to 0.0047 m s^{-1}. For NaOH and NaOH/NaCl, V_G varied between 0.0046 m s^{-1} and 0.031 m s^{-1}, with V_L fixed at 0.0089 m s^{-1}.

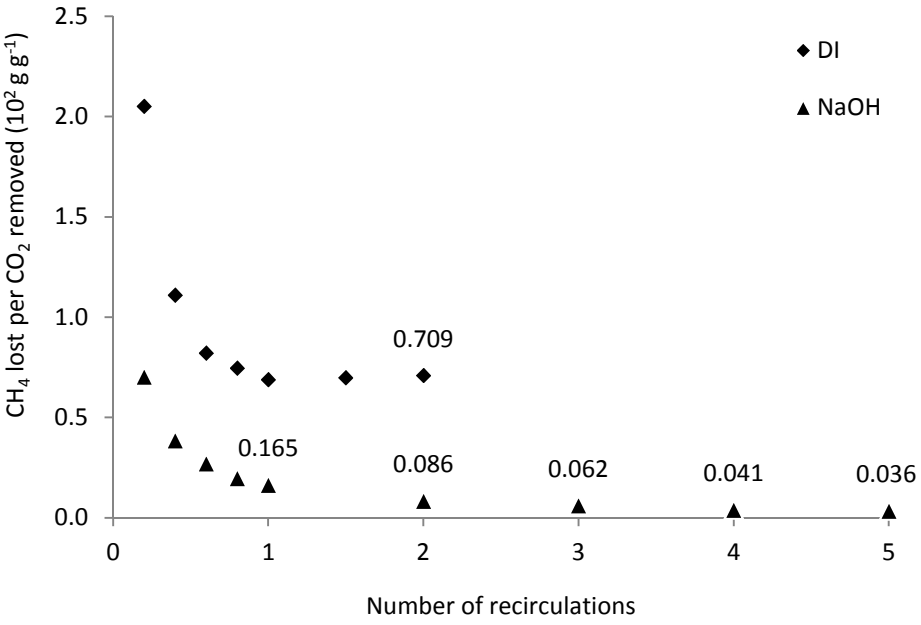

Figure 5. Methane losses measured over multiple solvent recirculations with DI or NaOH solvents. Methane losses normalised to CO_2 removed during gas separation. Operating L/G were selected that enabled effective CO_2 separation based on favourable CO_2 flux and gas-side purity. DI solvent V_l 0.024 m s^{-1} and V_g 0.0031 m s^{-1} (L/G 7.7); NaOH solvent V_l 0.032 m s^{-1} and V_g 0.058 m s^{-1} (L/G 0.42).

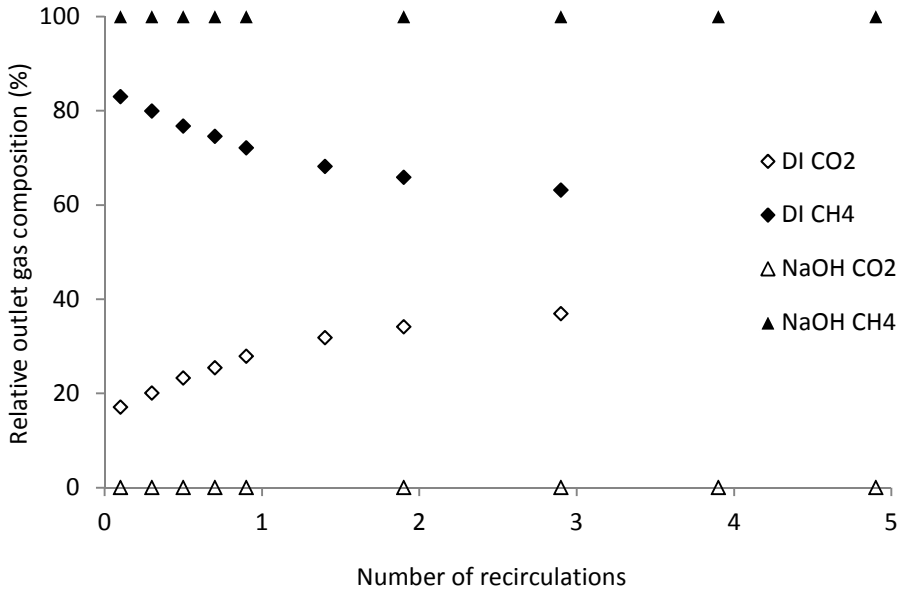

Figure 6. Outlet gas composition measured during sequential solvent recirculations using DI and NaOH absorption solvents. Solvent temperature 24-26 ˚C, V_l 0.024 m s^{-1} and V_g 0.0031 m s^{-1} for DI (L/G 7.7) and V_l 0.032 m s^{-1} and V_g 0.058 m s^{-1} for NaOH (L/G 0.42).

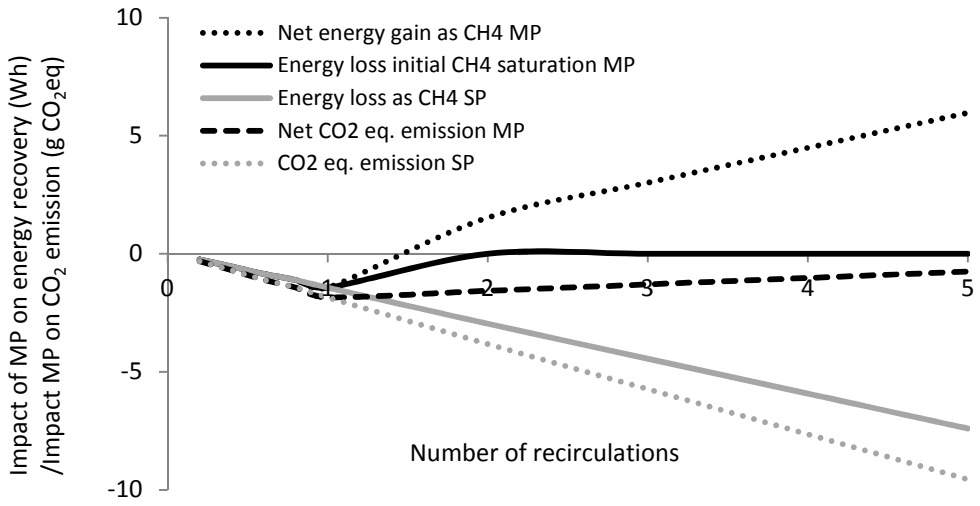

Figure 7. Energy and carbon balance based on methane slip during single pass (SP) and multi-pass (MP) solvent recirculation. A net energy gain is determined once solvent is recirculated more than once. Carbon neutrality requires greater than five solvent recirculations based on the modelled hydrodynamic conditions (assumptions 0.52 $kgCO_2$ kWh^{-1}; 40% electrical efficiency).

Table 1. Methane slip in DI, NaCl, NaOH, and NaOH + NaCl absorbents at 24-26 ˚C under conditions affording a relative output gas composition of 85 % CH_4.

Absorbent	L/G	Liquid velocity	Gas velocity	CH_4 slip	CH_4 slip vol.	Q_{CH4} out	CH_4 slip
	V_L/V_G	V_L, m s^{-1}	V_G, m s^{-1}	g m^{-3}	10^4 m^3 h^{-1}	m^3 h^{-1}	% CH_4 out
DI	5.18	0.0241	0.0047	16.0	5.8	0.011	5.22
1 M NaCl	5.00	0.0233	0.0047	9.6	4.1	0.010	4.00
1 M NaOH	0.33	0.0089	0.0300	10.0	1.3	0.136	0.10
1 M NaOH + 1 M NaCl	0.55	0.0089	0.0173	4.6	0.6	0.179	0.03